

Chapter 4

Speckle correlation technique for measurement of physical parameters

4.1 Introduction

This chapter deals with the application of the speckle correlation technique for the measurement of physical parameters such as temperature and magnetic field. Both these quantities serve as the fundamental physical parameters that are associated with many natural phenomena and industrial applications.

The operation principle of the proposed system is based on tracking laser speckle through a digital correlation technique [2,183]. It utilizes the speckle pattern produced by an optically rough reflecting surface when illuminated by laser light. The change in the measured quantity is determined by comparing the speckle pattern associated with its two different states. Standard cross-correlation methods [184] are used to determine translations of speckle fields over time, and it becomes clear that higher spatial bandwidth gives narrower cross-correlation estimates, resulting in more accurate lag parameters. Yamaguchi [185] has shown that by tracking speckle patterns emanating from surface elements illuminated by laser light, the surface element displacement can be calculated. The principle of tracking speckles works (resulting from stress due to temperature and magnetic field) by finding the correlation between speckle patterns is used here to measure the temperature and the magnetic field changes.

When a rough metal strip is exposed to temperature or magnetic field changes, speckle pattern resulting from the reflection of the laser beam, changes. This occurs due to the change in geometry of the metal plate undergoing temperature change and a pull due to the magnetic field. The intensity correlation between the speckle patterns at different temperatures/magnetic field [52,186] is then used to measure the temperature/magnetic field difference. The correlation function of the intensity between two points separated in the transverse plane by a radial distance of s and which are located at distance z from the diffusive object may be estimated as [187]:

$$\Gamma_{Transversal}(s) = \bar{I}^{-2} \left(1 + 2 \left| \frac{J_1(\pi\phi s / \lambda z)}{\pi\phi s / \lambda z} \right| \right) \quad (4.1)$$

where \bar{I} is the mean of the intensity in the output plane, ϕ is the diameter of the illuminating beam, J_1 is the Bessel function of the first kind, λ is the optical wavelength and z is the axial distance. It can be seen from the equation that as the temperature or magnetic field change s will change and hence the value of the correlation function changes. This change in correlation coefficient with temperature and the magnetic field is used for the measurement. In the practical system, temperature and magnetic field are determined by correlating the intensities of the speckle pattern recorded with the sensor head exposed to heat and magnetic field with a reference speckle pattern recorded without exposing the sensing head to these using the Eq. (2.8). The change in correlation coefficient was computed from the obtained correlation value using the Eq. (2.8).

4.2 Temperature Measurement

4.2.1 Introduction

When an object is heated or cooled, various effects may result including (a) changes in physical or chemical state, (b) changes in physical dimensions, (c) variations in electrical properties, (d) generation of an electromotive force (emf) at the junction of two dissimilar metals, and (e) changes in intensity of the total radiation emitted. Anyone of these effects can be employed for remote temperature measurement. Even though changes in the physical or chemical state provide a basic reference as temperature standard, e.g. freezing, melting, boiling or condensation of solids, liquids, or gases throughout the temperature ranges, they are seldom employed for direct temperature measurements. Another parameter that could give insight into the heat content of a body is the temperature at which a change in chemical state occurs, such as the ignition temperature of combustible materials. These can be utilized to determine the order of magnitude of the temperature scale, are not very practical. Bimetal and liquid in glass thermometers use the change in dimensions accompanying a temperature change for its measurement procedure. But electrical methods are by far the most convenient and accurate way of temperature

measurement. They include methods based on changes in resistance and generation of thermo emf. Temperature sensing, based on the method of measuring energy radiation from a hot object, is also a standard optical method of measurement, especially at very high temperatures [188]. In the field of temperature measurement, the knowledge of the temperature distribution has become crucial in many branches of science and engineering. With the development of modern technologies, new methods of temperature measurement have emerged, among which optical techniques play an important role, as they have incomparable advantages. One of the most important advantages of optical methods is that it can measure the temperature without disturbing the temperature field, which is in contrast to the intrusive measurement done by thermocouples [189]. Optical techniques exploit the change of the optical property that is caused by the change of the temperature to measure and calculate the temperature changes causing this change. There is a large number of optical techniques, such as, classical interferometry, holographic interferometry [190], speckle shearing interferometry [191], speckle photography [192], Talbot interferometry [193], shearing interferometry [194], Lau phase interferometry, Moire deflectometry[195], digital holographic techniques [196], effect mirage [197]and electronic speckle pattern interferometry (ESPI) [198], which are used mostly for room temperature tests. For high-temperature applications, the computer vision technique, ESPI, and the digital laser speckle correlation technique can be used [199]. But interferometric techniques suffer from problems of mechanical stability (due to vibrations) and in-plane and out-of-plane movements [199]. Holographic interferometric techniques provide full-field temperature data but they have extremely high sensitivity to vibrations; limiting its usefulness. These techniques also have the disadvantage of being integrating methods which require the deconvolution of the recorded data using some assumed symmetry in order to obtain temperature data for a specific point in space. It restricts the use of interferometry to a very limited number of phase objects because of the stringent optical conditions to be followed. Moreover, the obtained data should be mathematically processed to extract the numerical derivation of the phase shift which adds to the experimental error. Spectroscopic methods like spontaneous

Raman, spontaneous Raleigh scattering, coherent anti-Stokes Raman scattering spectroscopy (CARS), laser-induced fluorescence spectroscopy (LIFS), etc. provide a point by point data. Using these techniques thermal field can be mapped by integrating the region of interest point by point. Initially, Laser speckle was considered as noise in the imaging application which lead to low-quality images. But the speckle phenomenon became the steppingstone for the speckle metrology and it has been used in a variety of engineering and other applications [189,192,200,201]. For example, the digital laser-speckle technique is introduced into the measurement of the density field of the helium jet using the cross-correlation analysis of the speckle displacement, which provides high spatial-resolution in the measurement of density field in contrast to other optical techniques [200]. Therefore, further study of this optical technique is useful for application to the temperature measurement. Speckle correlation is one of several optical non-contact laser techniques available for measuring small surface displacements. Here, we propose a remote, non-contact approach for measuring temperature by imaging changes occurring to laser speckle patterns. When the aluminum (metal) strip is subjected to perturbations such as temperature, it experiences geometrical (size, shape) changes depending upon the nature and the magnitude of the perturbation. When coherent light is scattered or transmitted through an optically rough surface, secondary speckle patterns are generated [201]. The actual structure of the speckle pattern depends on the coherence properties of the incident field and also on the surface characteristics of the rough (target) object [176]. These two phenomena (change in physical properties and change in speckle field) are the backbone of the proposed sensor. The proposed temperature sensing device can be used for metrology related applications but also biomedical diagnostics. For instance, the proposed device can be integrated into an endoscope that can go into the body of the patient and estimate the temperature of internal organs e.g. for remote cancer detection or detection of internal inflammations.

4.2.2 Experimental procedure for temperature measurement

The optical arrangement is shown in Fig. 4.1 is used to determine temperature changes. A heating rod (3 mm diameter) is used to produce different temperature

distributions at the sensor head which is a metal (aluminum) cantilever. The heating rod is placed on a translation stage so that it can be adjusted to various distances from the sensor head leading to different temperature changes. The resulting temperature at the metal strip is also measured using a thermocouple which is used for the calibration purpose.

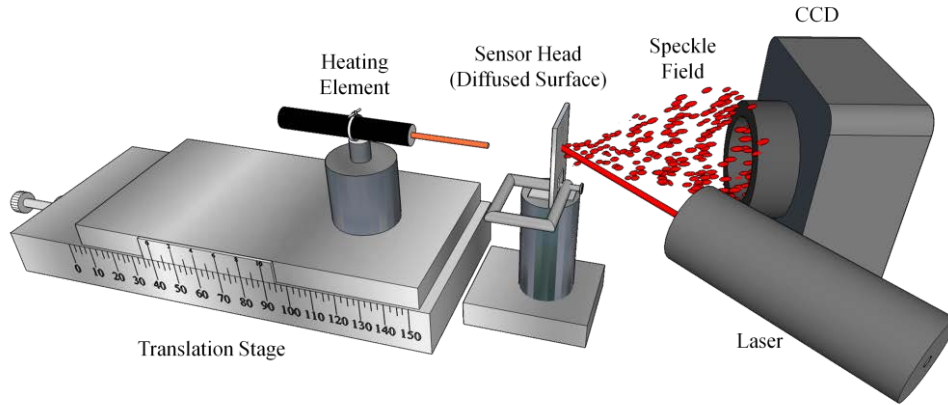


Fig 4. 1: Experimental configuration. The heating element was mounted on a translation stage

The illuminating light source consisted of He-Ne laser (randomly polarized, with $\lambda = 611.9$ nm, maximum output power < 2 mW) was illuminating a circular area of approximately 1 mm in diameter with a sufficient intensity to properly expose the CCD cameras or a laser diode beam, having approximately the same diameter, whose output power can be selected to be less than 2 mW. This may be of importance if such systems are used in the industrial environment. Due to the low power, special safety requirements are not necessary and it is easy to handle the sensor. The objective speckle field is sampled using a CCD camera (AVT Guppy-146 C, 8-bit dynamic range, $4.65 \mu\text{m}$ pixel pitch, 512×512 pixels exposed) connected to a PC. The proper exposure of the camera can then be controlled by a selectable electronic shutter or by introducing filters into the optical path. For this setup, the resolution of the displacement is physically limited by the wavelength λ used, the size of the laser spot illuminating the aluminum strip D and the pixel pitch of the CCD camera, as shown in Eq. (4.1). As already discussed, the

temperature measuring procedure consists of a continuous comparison of two speckle images. A reference speckle pattern is recorded at a known temperature. Other images are the scaled, displaced and possibly distorted version of this reference speckle pattern. The distortion can be caused either by any type of surface changes or due to the displacement of metal plate cantilever due to the change in the temperature.

4.2.3 Results and discussion

To test the applicability, the stability, the resolution and the limitations of the proposed optical temperature sensor, different temperature tests with different source locations (to get the different temperatures from the steady source) from the sensor head are carried, and the calibration plot is obtained from the given data. Before the calibration of the system is carried out, the ability of the technique to respond to temperature changes is checked. It is done by exposing the sensor head to the heating rod. Speckle patterns are recorded by the sensor at the rate of 1 Hz for different phases of heating. Fig. 4.2 shows the change in the speckle correlation coefficient as a function of time.

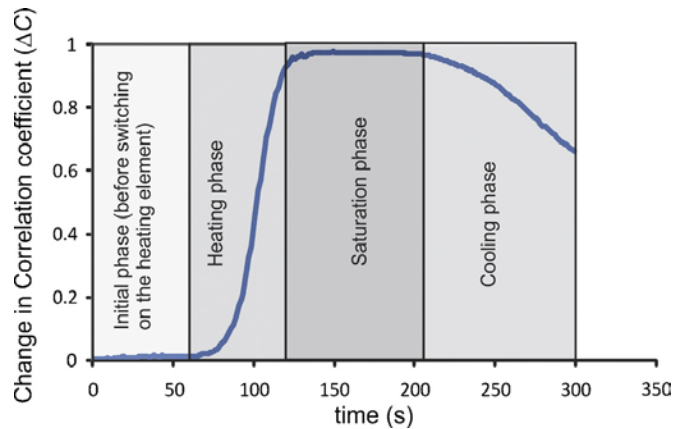


Fig 4. 2: Change in speckle correlation coefficient with time for heating element kept 1 mm away from the sensor head. Four regions are visible

A kernel of size 128×128 pixels, selected from the recorded intensity pattern is used to compute the correlation coefficient. It took 20 ms to compute one correlation coefficient using a PC with a Core i3 processor and 4GB RAM. Fig. 4.2 distinctly shows four regions: (1) initial phase, where there was no change as the

heat source was not switched on; (2) heating phase, where there is a sudden drop in the correlation coefficient or a sudden increase in correlation ΔC due to introduction of heat source; (3) saturation phase, at the maximum of the speckle correlation coefficient change (ΔC), indicating the maximum value of the speckle correlation and (4) cooling phase, where the speckle correlation coefficient change decreases again indicating that the sensor head is getting back to its initial state as the sensor (aluminum metal plate cantilever) gets cooled while reaching its initial temperature. This variation shows that the speckle correlation coefficient can be used to sense temperature changes. In the present technique, we used the heating phase and saturation phase for the measurement of temperature.

Calibration can be carried out either by comparison with a standard device whose accuracy is known or by using fixed points. The first method has the advantage that the test can be performed at any desired temperature, within the temperature range of interest, in a bath. The attainable accuracy depends on the uniformity of the temperature distribution in the test bath or the oven and the quality of the used reference standard. The reference standard should possess an accuracy of at least one order higher in magnitude than that of the sensor under the test. Calibration using fixed points allows the greatest possible accuracy attainable, but an elaborate setup is needed for each point. Here, the calibration of the system is done by comparing the change in correlation coefficient to the temperature measured with a thermocouple (Copper-Constantan) using the fixed-point method. The fixed point used is the triple point of water. This thermocouple is then used for the calibration of the sensor. Thermocouple has temperature range $73-673 K$, error limit 0.75% of the true value with a sensitivity of $15-60 \mu V / ^\circ C$ and accuracy of $\pm 1 ^\circ C$.

Sets of experiments are carried out using a heat source at different distances from the sensor head. First, a set of reference speckle patterns are recorded for 60 s. Heat source, whose temperature is to be determined is introduced behind the sensor head suddenly and the speckle patterns are recorded as a function of time. The object speckle pattern (recorded when the proposed sensor is exposed to the heat source)

is correlated to reference speckle pattern (recorded at some reference or known temperature) using Eq. (2.8) and the change in the correlation coefficient (ΔC) is calculated using Eq. (2.9). Object speckle patterns are recorded till there is no change in speckle correlation (or saturation in speckle de-correlation is reached). The frame rate is kept at 1 Hz during the recording process. Here, the sensor (aluminum metal strip) head is allowed to undergo the maximum change at a given temperature i.e. saturation value of change in correlation. Reference speckle patterns are recorded for all values of temperature changes (for different distances of the heating rod from sensor head) and the correlation coefficient is calculated as discussed above. Since the sensor is not taken away from the heating element after introduction, initially the change in speckle correlation is fast with time and then reaches a saturation value i.e. maximum change in sensor beyond which it cannot change. Variation in speckle correlation for various temperatures is shown in Fig. 4.3.

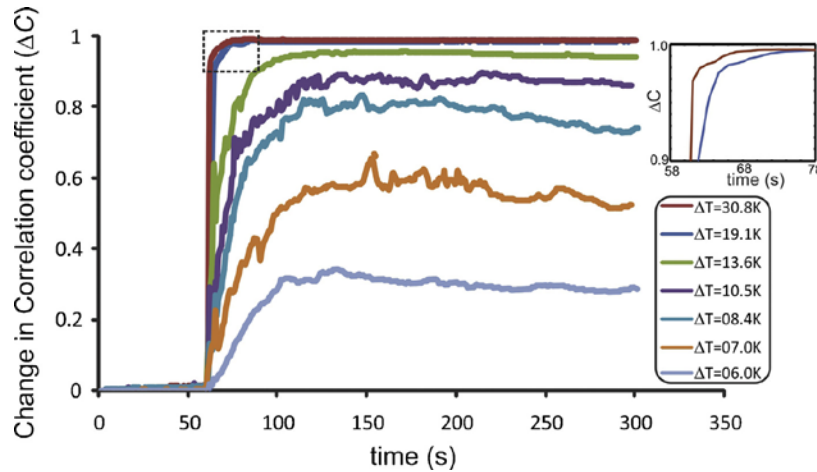


Fig 4. 3: Change in speckle correlation with time for heating element while the steady temperature was kept at different distances from the sensor head. The inset in the figure shows the expanded version of the region inside the rectangle

There are several possible ways for the measurement of temperature using this technique. The most obvious way is to use a saturation point, measure temperature from the maximum of the correlation change ΔC_{\max} in a given time when the sensor is exposed to heat source. Different distances from the heat source give different

temperatures at the sensor head, and it is expected to get different speckle pattern and thus the maximum change in correlation ΔC_{\max} values varies with the change in distance (indirectly due to different temperatures at sensor head). The calculated ΔC_{\max} is then plotted versus the applied temperature of the heat source. But ΔC_{\max} does not change much at higher temperature variations, so it is not ideal for temperature determination as can be seen from Fig. 4.3 where, at high temperatures the (ΔC) lines almost overlap. Another way to measure the temperature is, by finding the slope of the t versus ΔC curve for heating phase and to plot it as a function of the temperature. Fig. 4.4 shows the slope of change in correlation with time (heating phase of Fig. 4.2) and plotted as a function of temperature. The slopes were computed after linearly fitting the curve separately for heating regions at different temperatures.

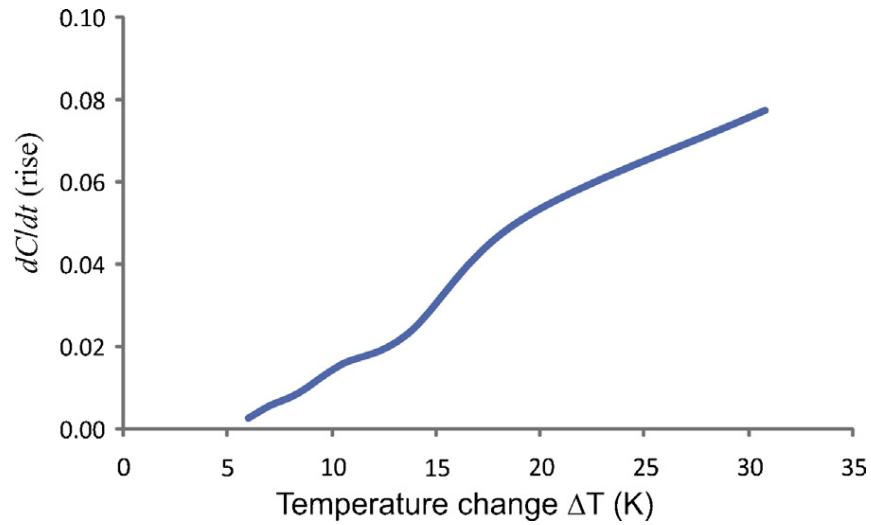


Fig 4. 4: Slope of the ΔC versus ΔT during heating (saturation region is not considered)

This curve can then be used to determine the temperature. For the maximum change of temperature $\Delta T = 30.8 K$, the slope of the ΔC versus ΔT changes by an amount of $0.0775 s^{-1}$ which computes the sensitivity of $0.0025 s^{-1} K^{-1}$. For the minimum temperature change of $6 K$ the sensitivity comes out to be $0.0004 s^{-1} K^{-1}$. The third way, in which the data could be analyzed, is by determining the

time taken for the sensor head to reach its saturation value (ΔC_{\max}). This can be determined from the width of the t versus dC/dt curve as shown in Fig. 4. 5.

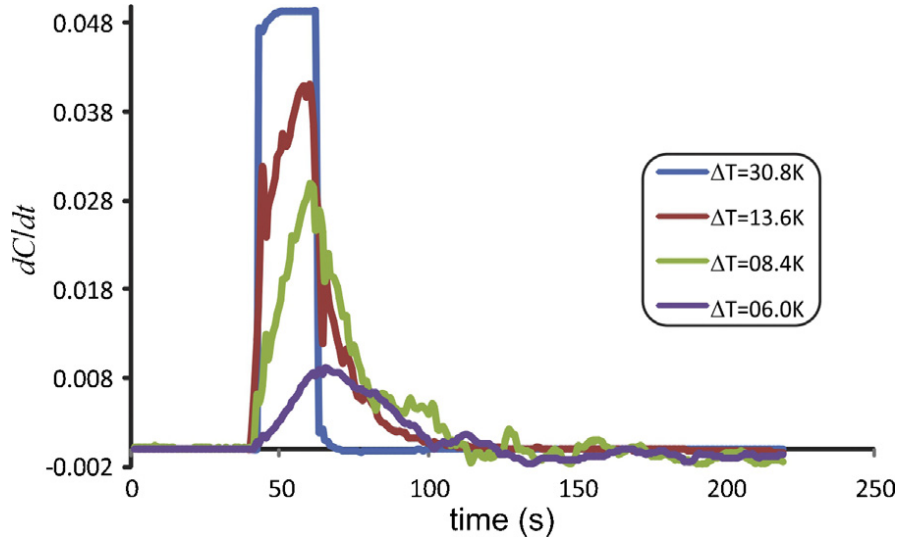


Fig 4. 5: Variation in the slope of C as a function of time. This can be used to determine the time it takes the sensor head to reach saturation

The time that the sensor head required to reach the saturation point as a function of the change in temperature ΔT is shown in Fig. 4.6. Here, the curve has two regions separated by ΔT value of around 16 K (absolute temperature of 319 K)

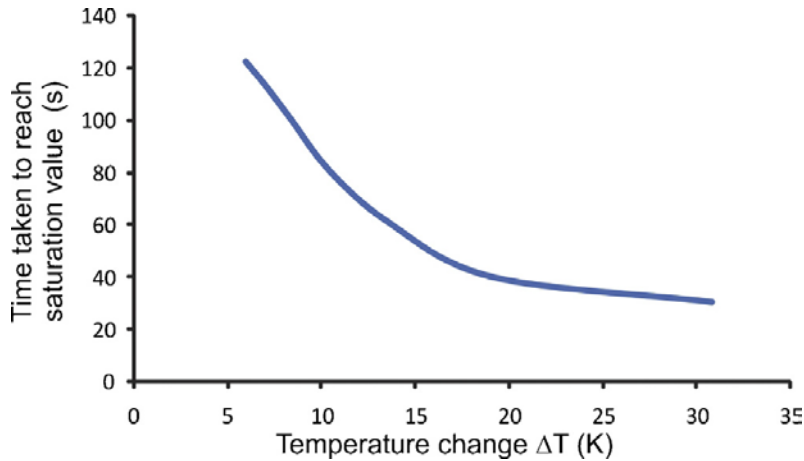


Fig 4. 6: Change in the time it takes the sensor head to yield saturation in the speckle correlation values as a function of the change in the temperature

This curve can then be used to determine the temperature. For the maximum change of temperature $\Delta T = 30.8 \text{ K}$, the time taken by the sensor head to reach saturation was 30.8 s which results with a computed sensitivity of $0.9997 \text{ S } K^{-1}$. For the minimum temperature change of 6 K , sensitivity comes out to be $20.4 \text{ S } K^{-1}$. The accuracy of the system is determined statistically, by performing a similar set of experiments under the same environment. True value is taken as the average value from the statistical procedure and accuracy of the system is determined. In both cases, the accuracy of the system in the measured range was found to be better than 1 K . From the curve shown in Fig. 4.2, it can be seen that the sensor takes a finite time to get back to the initial state. The cooling time of the sensor is determined by removing the heating source after the correlation coefficient has reached its saturation value and then finding the time after which the correlation value reaches its initial minimum value. It is found that on an average sensor takes 19 s to cool and return to the initial state.

4.3 Magnetic Field Measurement

4.3.1 Introduction

Many essential and fundamental parameters play a critical part in sustaining and evolving life on this planet. One of them is the magnetic field which is related to a large number of natural phenomena. Thus, it would be of great interest to accurately measure such significant parameters and develop necessary tools and techniques to measure it [202]. From the earliest times, the measurement of magnetic fields generated by earth's magnetic poles has helped in navigation during distant journeys over vast oceans. In the last few decades, magnetic field sensors have grown by leaps and bounds and are playing an important role in various fields such as navigation, military, industrial and electric power transmission, biomedicine, multimedia [203–211]. An increase in productivity is witnessed in the industries due to the increase in the reliability and stability of magnetic sensors [212–214].

Magnetic field sensors can be classified into a vector component and scalar magnitude types. Magnetic sensors measuring vector components can further be

divided into sensors that can measure low field (<1 mT) and high field (>1 mT). Low field measurement sensors are known as magnetometers while the high field measurement sensors are called gaussmeter [215,216]. For sensing fields that lie between low field and high field, the magnetoresistive sensors are used, where anisotropic magnetoresistors (AMR) are currently being used for various applications including magnetometers. The development of giant magnetoresistive (GMR) check effect improved sensitivity which helped in achieving results comparable to the traditional fluxgate magnetometer in the medium-sensitivity applications[217].

Various methods for magnetic field measurement based on different physical effects have been presented [218–223]. Sensors based on several magnetic effects such as Hall effect [209,224], magnetostrictive effect [223], magnetic moment [225], magneto-optic effect [226], fluxgate sensors [227], Superconducting quantum interference devices (SQUIDs) [228], have been reported[217]. The Hall Effect device is one of the oldest and most commonly used gaussmeters for measuring the high magnetic field. The induction coil and fluxgate magnetometers are the most extensively used vector measuring instruments as they are rugged, reliable and relatively less expensive than many low field vector measuring instruments. The SQUID magnetometers are one of the most sensitive of all magnetic field measuring instruments it is more expensive, less rugged and less reliable as it operates at temperatures near absolute zero and requires special thermal control systems [217].

The task of geometrical exploration and aerial mapping of the geomagnetic field is accomplished by employing the proton (nuclear) precession magnetometer, which measures scalar magnetic field strength. It further can be used as the primary standard for calibrating magnetometers as its works on the principle of fundamental atomic constants. But it cannot measure fast changes in the magnetic field owing to its very low sampling rate (1 to 3 samples per second). To measure fast changes

in the magnetic field, optically pumped magnetometers are used which operate at a higher sampling rate but are more expensive, less rugged and less reliable [217].

Preferring optical sensors over the conventional electrical or electromagnetism based sensors has been proved to be very advantageous as the optical sensors are non-contact and provide high sensitivity and immunity to electromagnetic interference [202,208,217]. Optical sensors employing Optical fiber is one such modality that is less susceptible to electromagnetic interference and is lightweight [229]. The detection of the magnetic field is realized by combining optical fibers with magnetic materials such as magnetic fluid (MF), a colloid that contains magnetic nanoparticles dispersed in a suitable liquid carrier such as water, oil or ester [230]. A fiber optic sensor comprises of a sensing element which modulates light when it is acted upon by a physical quantity. Optical fibers guide the light to and from the sensing element. Intensity-based sensors are designed to detect changes in the optical system which are induced due to many reasons such as moving parts [231], optical loss (environment dependent) [232], microbendings in optical fiber [233,234], reflections from gratings [235], scattering due to temperature fluctuations in optical fiber [236], losses due to impurities and improper light decoupling in case of optical fiber [237], etc.

In this work, a remote, non-contact approach for measuring static as well as alternating magnetic fields (of the order of microtesla) by laser speckle de-correlation technique is presented.

It is already discussed in the case of temperature measurement that when a laser beam is scattered from an optically rough surface of the sensing element (metallic strip), the speckle pattern is generated. The shape and size of the speckle pattern depend on the coherence properties of the incident light and characteristics of the rough surface [176]. Any deviation in the position of the sensing element under the influence of the magnetic field is reflected as a change in the correlation coefficient of the speckle pattern. Thus, the relation of speckle pattern with the varying physical quantity serves the basis of the proposed sensor.

4.3.2 Measuring the magnetic field without using the speckle correlation technique

To demonstrate the effectiveness of the speckle correlation technique, an experimental setup that comprises an LED (650 nm, operating at 2.5 V and 153 mA) source and a photodiode is used instead of imaging laser speckle pattern to measure the magnetic field. The optical arrangement is as shown in Fig 4.7.

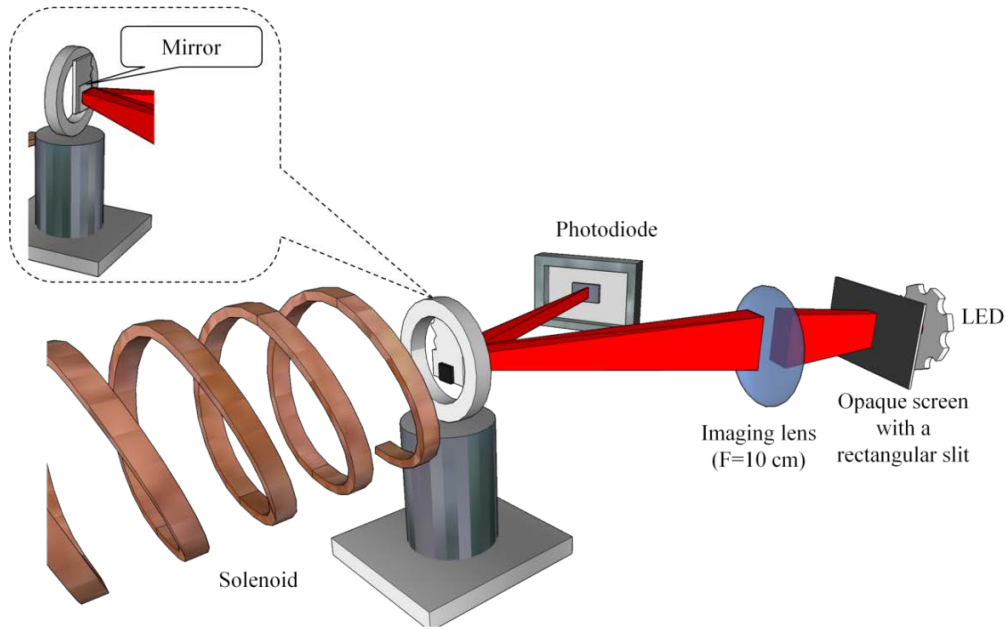


Fig 4. 7: Experimental setup for measuring magnetic field without using the speckle correlation technique

The sensor head comprises a small mirror attached to a bar magnet which is connected at the lower end of the metal strip (razor blade), whose upper end is connected to a fixed base. As the metal strip is fixed at one end and free at the other, it can be considered as a cantilever. When the magnetic field is applied to the sensor head, a force is exerted at the free end of the metal strip where the bar magnet is attached. Due to this, the cantilever changes its initial (straight) position and bends (into a curve) [217]. The differential equation of the deflection curve of a cantilever is given by [238]:

$$\frac{d^2v}{dx^2} = \frac{M}{El} \quad (4.3)$$

where v is the displacement of the cantilever, M is the bending moment and EI is the flexural rigidity (resistance of a beam to bending). The light from the LED is allowed to pass through a rectangular slit and the image of this slit is made to fall in the photodiode after specularly reflecting it from the mirror which is placed on the sensing head as shown in the Fig. 4.7. Thus, a change in the position of the cantilever will bring about a lateral shift in the position of the image of the slit on the photodiode. This lateral shift leads to varying output voltage. To optimize this effect, initially, the focused image is allowed to fall at the edge of the photodiode and on applying the magnetic field the focus shift towards the center of the photodiode which increases the output voltage as shown in Fig. 4.8.

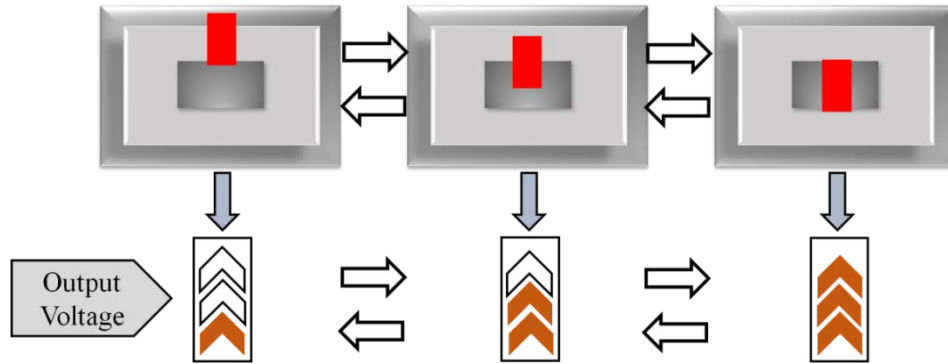


Fig 4. 8: Movement of focused image on the photodiode when magnetic field varies

The system is calibrated by applying the static magnetic field ranging from 0G to 10G in the step of 0.48G at the sensor head and noting the corresponding change in the output of photodiode. The experiment is repeated 10 times. The output data of the photodiode is averaged over 10 trials and the calibration plot is obtained. The variation of photodiode output as a function of the applied magnetic field, which acts as a calibration curve is graphically shown in Fig. 4.9.

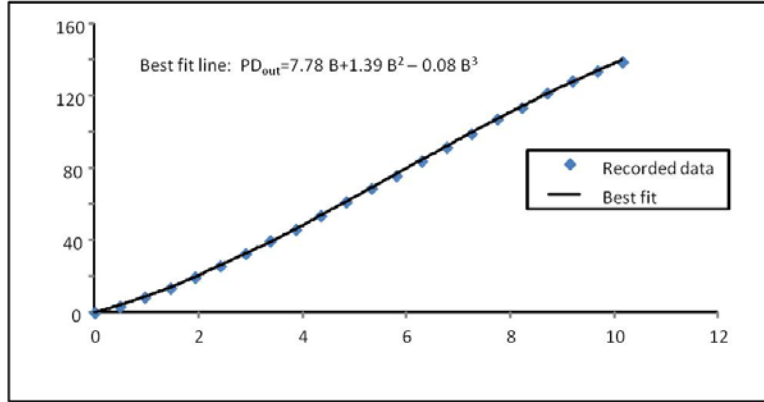


Fig 4. 9: Calibration curve giving the relation between the magnetic field and the output of the photodiode

From the best fit of the obtained data (Fig. 4.9), we get the calibration equation which can be used to measure unknown magnetic fields. It can be seen from Fig 4.9 that the curve is quadratic which reflects the cantilever form of the sensing element.

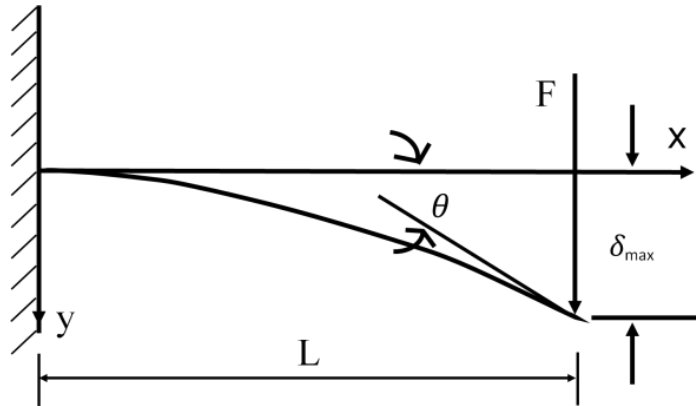


Fig 4. 10: Cantilever action for one fixed and one open end

For a cantilever fixed at one end as shown in the Fig. 4.10, the deflection at a particular position is linear with respect to the applied load (here magnetic field) and the relationship between the deflection and the position at which the deflection is measured is given by [238]:

$$\delta_x = \frac{Fx^2}{6EI}(3L - x) \quad (4.4)$$

where δ_x is the deflection, F is the load acting on the beam of length L , EI is the flexural rigidity and x is the distance from the fixed point. It is very evident from Eq. (4.4) that the deflection δ_x is proportional to x^3 which is in agreement with the calibration curve shown in Fig. 4.9.

The ability of the system to measure the unknown magnetic field is tested by applying the magnetic field from 1G to 9G in the steps of 1G. For each value of the magnetic field, the output of the photodiode is recorded. Then, the obtained photodiode output is used in the calibration plot to measure the applied field. Fig. 4.11 graphically shows the variation in the measured magnetic field as a function of the applied magnetic field. The plot also shows the percentage error for each measurement.

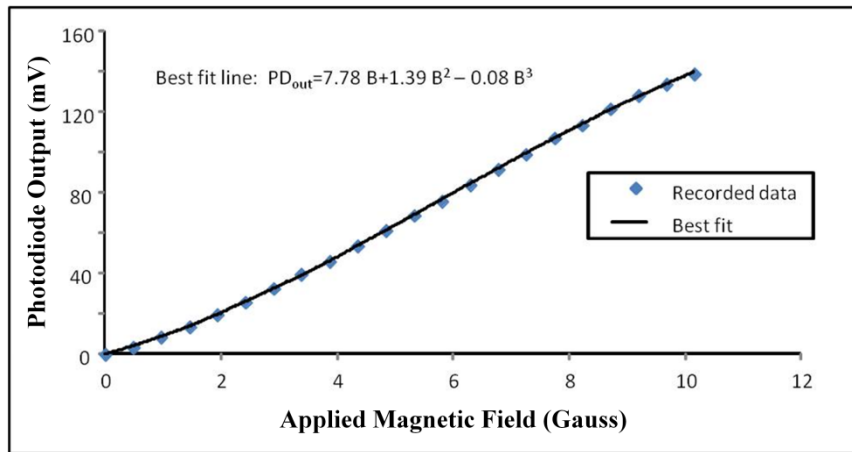


Fig 4. 11: Measured magnetic field along with percentage error

The sensitivity gives information about the response of the system with the change in measured quantity. In the presented system it is obtained by taking the difference between the consecutive values of the output of photodiode and averaging it over the applied magnetic field difference (0.48G). The sensitivity turns out to be 13.99 mV/G. The resolution of the system is calculated from the average of the standard deviation of the voltage values obtained over corresponding magnetic field values. The average of the standard deviation turns out to be 1.24 mV, which when used in

the calibration curve provides the value for resolution of the system. The resolution of this optical arrangement turns out to be 0.15G. Since the motivation behind carrying out this set of experiment was to validate the utilization of the mechanical movement of a cantilever in measuring magnetic field, repeatability of this particular optical arrangement is not explored. A detail study will be carried out in the next section where the speckle correlation technique will be employed.

Hence it is proved that the concept of using cantilever effectively measures the magnetic field and now we can proceed to the speckle correlation technique for further enhancing the measurement efficiency and resolution.

4.3.3 Experimental Setup and Procedure

The schematic of the optical arrangement for the measurement of the magnetic field using the speckle correlation technique is shown in Fig. 4.12.

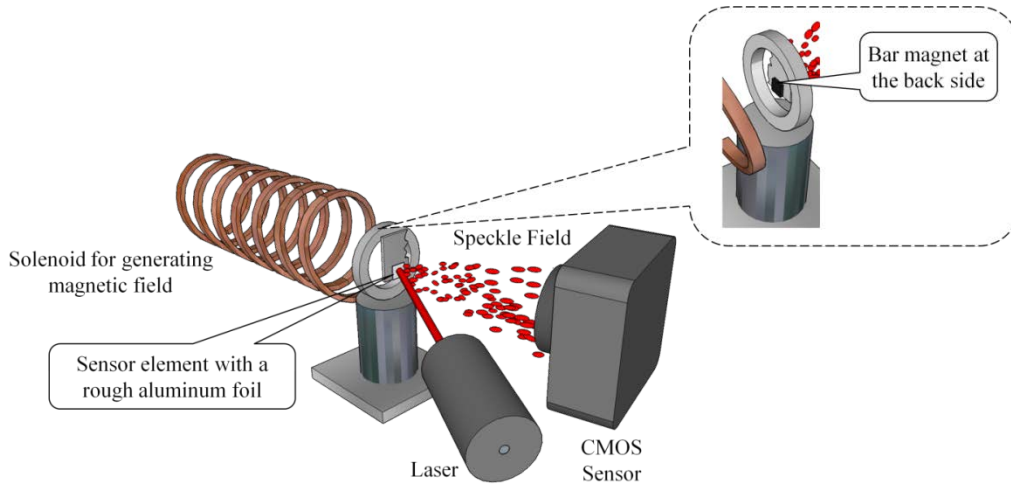


Fig 4. 12: The Schematic of the experimental setup for measuring the magnetic field

The sensing head comprises a strip of a razor blade, aluminum foil (6.5mm X 5mm X 3mm) and a bar magnet (3 Kilogauss). One end of the strip of the razor blade is attached to a fixed point while its other end is kept unattached. The optically rough aluminum foil is affixed to the free end of the cantilever on which the unexpanded laser is allowed to fall to create the speckle field upon reflection. The speckle pattern is recorded using a CMOS sensor. To enhance the system's ability to sense

small changes in the magnetic field a bar magnet is attached at the rear side of the cantilever as shown in the inset of Fig. 4.12.

This cantilever arrangement that forms the sensing head is placed at one end of the solenoid (electromagnet) to apply magnetic fields of different strengths. Many sets of experiments are conducted for selecting the most appropriate material which can be used as a cantilever. Objects such as spring, double spring, paper, foil and razor blade strip are used, out of which the razor blade produced results with good precision and accuracy, and thus is selected as the cantilever object. A randomly polarized He-Ne laser (unpolarized, 611.8 nm, maximum output power <2 mW) is used as the light source which illuminates a circular area of approximately 1 mm in diameter at the aluminum foil, while a CMOS sensor (Intex VGA webcam with 3.2 μm pixel pitch and 640 \times 480 pixels exposed) is used to record speckle patterns. To make the system applicable to the industrial environment the He-Ne laser can be replaced by a laser diode having approximately the same beam diameter and output power. As the power of the source used here is low, special safety measures need not be necessarily taken care of.

4.3.4 Results and Discussion

Before engaging the system to measure the magnetic field, the system is calibrated using the known magnetic field and the system's response to the magnetic field is observed. The calibration of the system is carried out by applying magnetic fields ranging from 15.6 mG to 312 mG in the step of 15.6 mG and computing the respective change in the correlation coefficient. The correlation coefficient is computed by comparing the speckle pattern associated with the applied magnetic field with the speckle pattern associated with the state where no magnetic field is applied. Here, the speckle pattern corresponding to the zero magnetic field is considered as a reference level. Two sets of data at 7 fps for 3 s are recorded for each value magnetic field; one for the reference level of the magnetic field and the other for the known value of the magnetic field. The correlation coefficient values (ΔC) for each value of the applied magnetic field are computed using Eq. (2.8) and the change in correlation values is obtained using Eq. (2.9). The same

procedure is repeated 20 times for the complete range of magnetic field and an average value of correlation coefficient value for each magnetic field is computed. Fig. 4.13 is the calibration curve which is used during the experiment. The average standard deviation over each value of the magnetic field for all trials represents the repeatability of the system. This repeatability is considered as the system's resolution which turns out to be 4.4 mG .

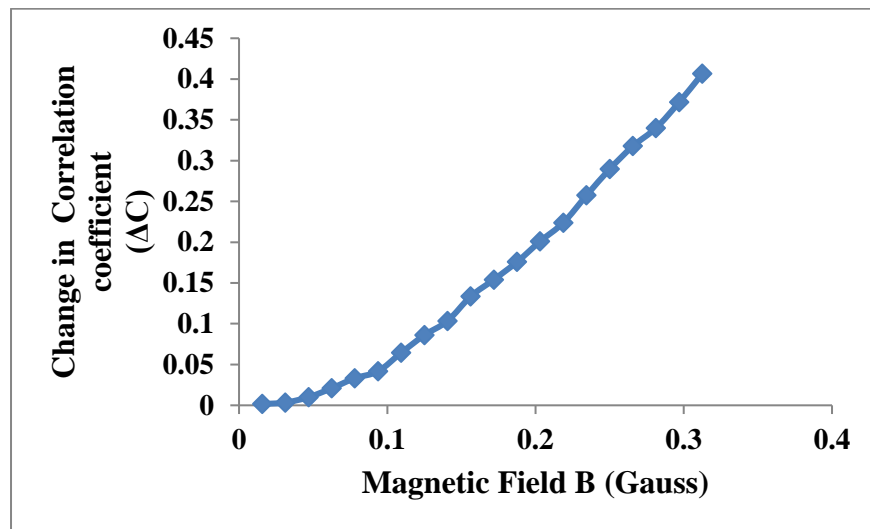


Fig 4. 13: Change in the speckle correlation coefficient (ΔC) for magnetic field variation from 15.6 mG to 312 mG in the step of 15.6 mG

The time taken by the sensing head to sense and respond to the applied magnetic field can be considered as the response time of the system. To determine the response time a sequence of the speckle pattern is recorded for 5 s and the magnetic field (172 mG) is applied for the last two seconds of the recording. It can be seen from Fig. 4.14(a) there are two distinctively separated regions (1) before applying the magnetic field (2) after switching on the magnetic field. The system takes 3 frames to respond to the applied magnetic field thus the response time is computed and is 430 ms .

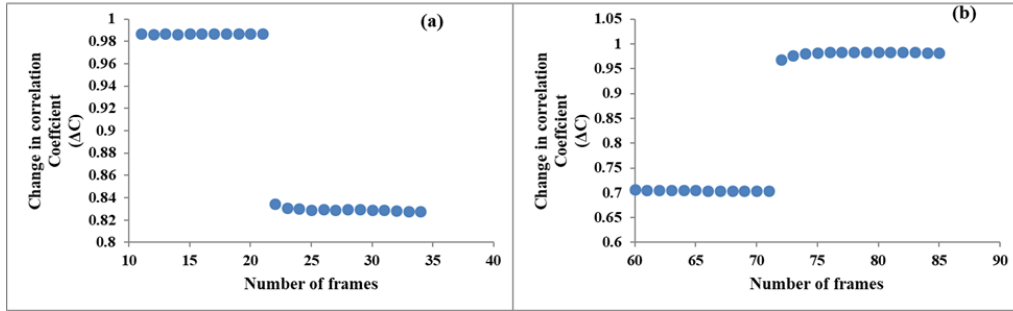


Fig 4. 14: Correlation coefficient (a) Response time (b) Recovery time

The recovery time of the system is the time taken by the system to reach its initial position after switching off the magnetic field. To determine the recovery time a sequence of the speckle pattern is recorded for 5 s where the magnetic field (234 mG) is applied from the beginning of the recording and it is switched off suddenly after 2 s. It can be seen from Fig. 4.14(b) there are two distinctively separated regions (1) while the magnetic field is applied (2) after switching off the magnetic field. The cantilever takes 430 ms to reach its initial position after switching off the magnetic field.

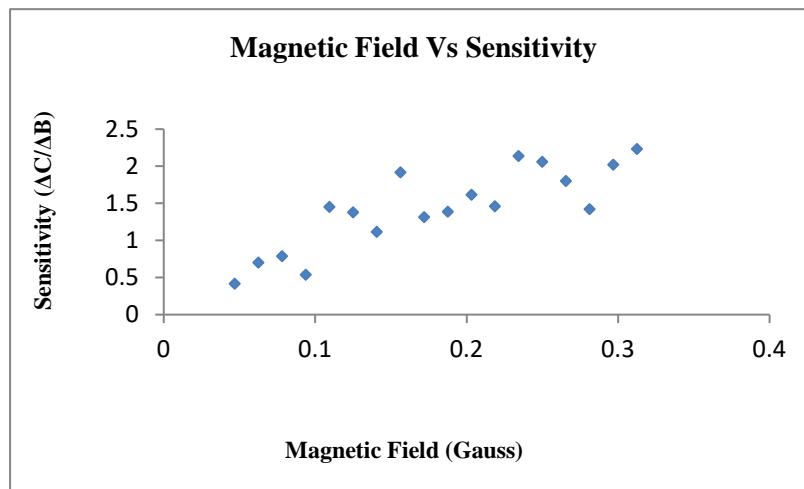


Fig 4. 15: Variation in sensitivity with the applied magnetic field

The system's sensitivity is defined as the amount of change in the correlation coefficient upon a unit change in the applied magnetic field. The average sensitivity of the system over the range of the magnetic field used in the calibration process is

computed to be 1.433 ($\Delta C / \Delta B$) i.e. a magnetic field of 1 G changes the correlation by 1.433, which is not theoretically possible as the maximum change in ΔC value can be 1. This indicates that the system has high sensitivity. The plot of the magnetic field versus the sensitivity is shown in Fig. 4.15. It is very evident from Fig. 4.15 that as the strength of the magnetic field increases, the sensitivity of the system also increases.

Five different values of the unknown magnetic field were applied to the system and the calibration plot is used for the measurement procedure. Table 4.1 shows the percentage error in the measurement of the magnetic field by comparing the measured magnetic field

Table 4.1 shows the performance of the system in measuring the magnetic field, where the measured magnetic field is compared with the theoretically calculated magnetic field and the respective percentage error has been obtained. It is observed that the average error in the system turns out to be less than 7%.

Table 4. 1: Measurement of static magnetic field

Magnetic Field (Theoretically Calculated)	Magnetic field (Experimentally determined)	Percentage Error
0.0366	0.32226	11.95
0.04706	0.047486	0.90
0.0549	0.055421	0.94
0.062448	0.056071	10.21
0.073201	0.080789	10.36

After successfully demonstrating the system's ability to measure static magnetic field, measurement of alternating magnetic field is carried out. It is already established that the system's response and recovery time is 430 ms, and thus according to the Nyquist sampling criteria, theoretically the developed system can only measure frequencies equal to or less than 1.16 Hz (≈ 1 Hz). Thus to explore

the system's ability to measure alternating magnetic field, frequencies of 0.5 Hz and 1 Hz are used.

A sinusoidal frequency generator is used to produce the required alternating magnetic field of different strengths by varying the current supplied to the solenoid. Two sets speckle pattern are recorded for 14 s each at 7 fps. The first set of data for reference level is recorded for the speckle patterns corresponding to state of no applied magnetic field. Initially the alternating magnetic field with five different magnitudes (corresponding to 5 mA, 7 mA, 9 mA, 11 mA, and 14 mA of current through the solenoid) with frequency of 0.5 Hz is used. The second set of the speckle patterns is recorded for 14 s in which (a) no magnetic field is applied initially for 2 s (0 to 2 s) and (b) alternating magnetic field is applied for next 8 s (2 to 10 s). Then the magnetic field is switched off and the speckle patterns corresponding to this state are recorded for 4 s (10 to 14 s). The correlation coefficient and corresponding change in correlation coefficient (ΔC) is computed using Eq (2.9) and Eq. (2.10).

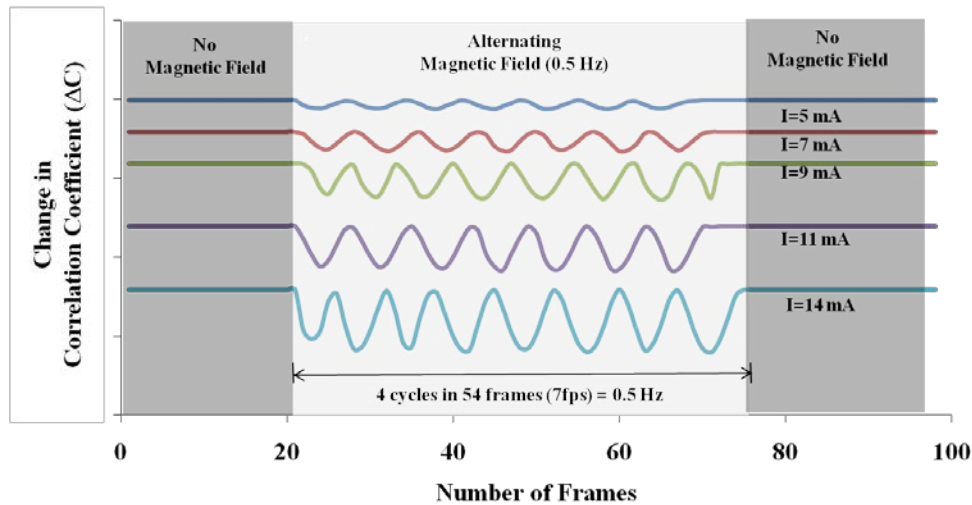


Fig 4. 16: Change in correlation coefficient with number of frames for different values of magnetic fields oscillating at 0.5 Hz

Fig 4.16 shows the change in correlation coefficient with the number of frames for different magnetic fields oscillating at 0.5 Hz. The alternating magnetic field is applied for 8 s and it is evident from the plot that the system is able to measure the applied frequency satisfactorily. To obtain the values of the applied magnetic field

RMS values of the correlation coefficients values were computed and were plugged in the calibration curve.

Table 4. 2: Measurement of alternating magnetic fields at 0.5 Hz

Applied Magnetic Field (G) (0.5 Hz)	Change in Correlation Coefficient (ΔC) (RMS value)	Magnetic field obtained using Calibration Curve (G)	Percentage Error
0.078134	0.033568	0.071234	8.83
0.109387	0.063621	0.10964	0.23
0.14064	0.10744	0.152846	8.68
0.171894	0.136162	0.17669	2.79
0.218774	0.196302	0.219811	0.47

Table 4.2 shows the performance of the proposed system in measuring the alternating magnetic field where it is compared with the theoretically calculated magnetic field and the percentage error has been obtained. It is observed that the average error turns out to be less than 5%.

Similarly, various values of magnetic field oscillating at 1 Hz are applied to the system and its response is presented in Fig. 4.17. The alternating magnetic field with five different magnitudes (corresponding to 6 mA, 8 mA, 10 mA, 12 mA, and 14 mA of current through the solenoid) with frequency of 1 Hz are used in this measurement. It can be seen that, as the current in the solenoid increases the amplitude of the oscillations also increases which is reflected from the increased RMS values. Table 4.3 shows the measurement of five different alternating magnetic fields and the computed percentage error.

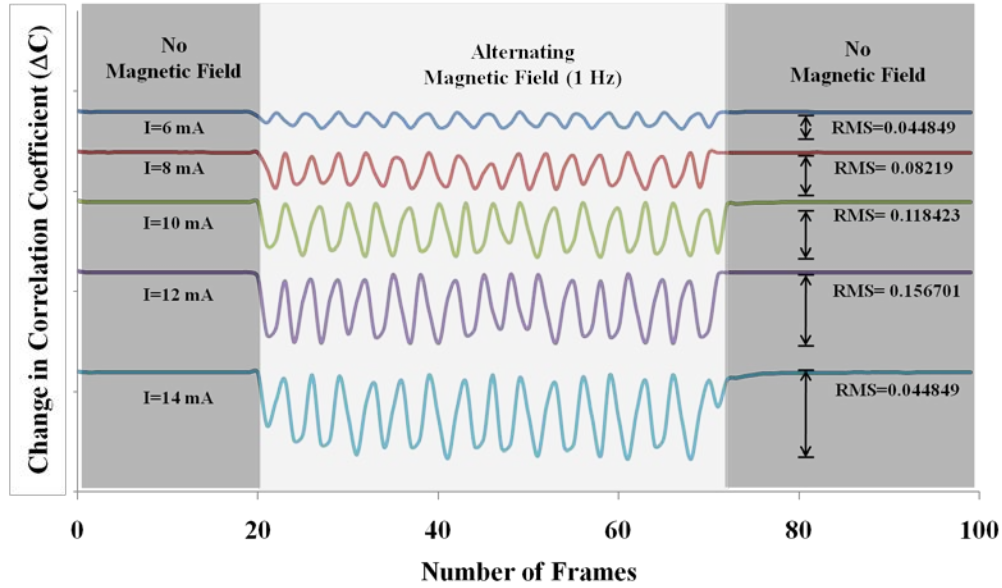
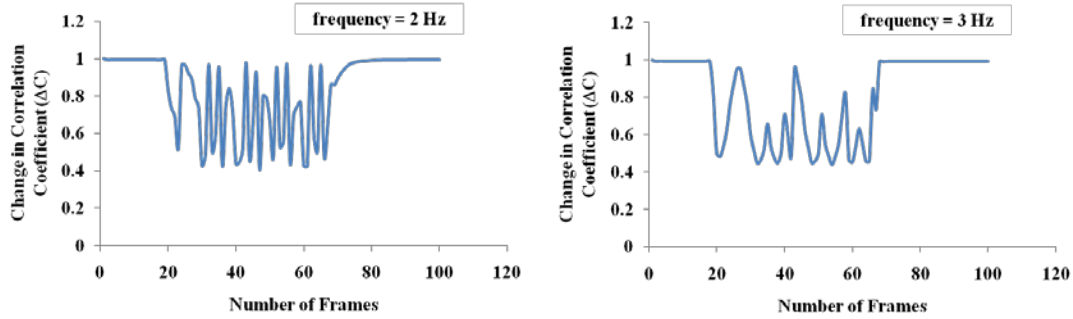


Fig 4. 17: Change in correlation coefficient (ΔC) with number of frames for different values of magnetic fields oscillating a 1 Hz

Table 4. 3: Measurement of alternating magnetic fields at 1 Hz

Applied Magnetic Field (G) (1 Hz)	Change in Correlation Coefficient (ΔC) (RMS value)	Magnetic field obtained using Calibration Curve (G)	Percentage Error
0.09376	0.044849	0.086944	7.27
0.125014	0.08219	0.129244	3.39
0.156267	0.118423	0.162284	3.85
0.18752	0.156701	0.192291	2.54
0.218774	0.195017	0.218963	0.08

To validate the theoretical conclusion that the system only measures frequencies less than 1.16 Hz (1 Hz), frequencies of 2 Hz and 3 Hz were applied to the system and corresponding response of the system in terms of change in correlation coefficient is presented in Fig. 4.18.



4. 18: Change in correlation coefficient (ΔC) with number of frames for frequency of 2 Hz and 3 Hz

It can be clearly seen from Fig. 4.18 that the system is not able to respond to higher frequencies and provides incorrect frequency due to under-sampling.

4.4 Conclusion

The work described here is dedicated to the development of speckle correlation techniques for quantifying physical parameters such as temperature and magnetic field. Both these parameters are measured with different optical arrangements with some similarities. Both the optical arrangements use a physical change of a metal strip to convert the change in the measured quantity into a change in the speckle pattern. The optical arrangements use objective speckle pattern and are non-contact in nature. The laser-based non-contact sensor can be an attractive alternative to commercial sensors that are not immune to electromagnetic interferences and of contact type. The optical arrangements can be made very compact by employing a diode laser instead of a gas laser and a webcam sensor instead of CCDs. This can also reduce the cost of the system. The compact nature of the system may prove to be beneficial while incorporating this system in biomedical devices, especially for temperature measurement. An optical arrangement for measuring magnetic field that does not utilize speckle correlation technique was also explored and the results are compared to that obtained by the measurements done using speckle correlation technique. It is observed that the laser speckle correlation technique provides much better resolution.

The size of the speckle pattern will decide how fast the de-correlations happen. Therefore, to increase the range one can use a laser beam with smaller spot size,

thereby increasing the speckle size at the detector resulting in a slower change in speckle de-correlation and hence can sense over a larger range. The main limitation of the technique includes higher sensitivity to the environment (causing unwanted vibrations of the sensor metal plate), which might result in the wrong measurement and it is required to take reference every time as well as from the measured quantity.

In the future, possible applications to be explored will include the implementation of this concept for biomedical monitoring in which in-body or in-tissue thermal variations can be extracted in a minimally invasive manner while the principle of the proposed device is incorporated as part of a biomedical endoscope. The possibility of integrating the proposed sensor with smartphones (which may have both the camera as well as the laser diode) will also be explored.